AN APPLICATION OF 3-D KINEMATICAL CONSERVATION LAWS: PROPAGATION OF A THREE DIMENSIONAL WAVEFRONT

K. R. ARUN, M. LUKÁČOVÁ-MEDVIĎOVÁ, PHOOLAN PRASAD, AND S. V. RAGHURAMA RAO

Abstract. 3-D kinematical conservation laws (KCL) are equations of evolution of a **propagating** surface Ω_t in three space dimensions and were first derived in 1995 by Giles, Prasad and Ravindran [15] assuming the motion of the surface to be isotropic. We start with a brief introduction to 3-D KCL and mention some properties relevant to this paper. The 3-D KCL, a system of 6 conservation laws, is an under-determined system to which we add an energy transport equation for a small amplitude disturbance to study the propagation of a three dimensional nonlinear wavefront in a polytropic gas in a uniform state and at rest. We call the enlarged system (3-D KCL and the energy transport equation) equations of weakly nonlinear ray theory - WNLRT. We highlight some interesting properties of the eigenvalues of the equations of the WNLRT but main aim of this paper is to test the numerical efficacy of this system of 7 conservation laws. We take initial shape of the front to be cylindrically symmetric with a suitable amplitude distribution on it and let it evolve according to the 3-D WNLRT. The 3-D WNLRT is a weakly hyperbolic 7×7 system that is highly nonlinear. Due to a possibility of appearance of δ waves and shocks it is a challenging task to develop an appropriate numerical method. Here we use the Lax-Friedrichs scheme and Nessyahu-Tadmor central scheme and have obtained some very interesting shapes of the wavefronts for two cases - in one case kink lines and another case a point singularity appear in the physical space though the results remain single-valued in the ray coordinates. Thus we find the 3-D KCL to be suitable to solve many complex problems for which there seems to be no other method which at present can give these physically realistic features.

1. Introduction

Propagations of a nonlinear wavefront and a shock front in three dimensional space $\mathbb{R}^3$ are very complex physical phenomena and both fronts share a common property of possessing curves of discontinuities across which the normal direction to the fronts and the amplitude distribution on them suffer discontinuities. These are discontinuities of the first kind, *i.e.,* the limiting values of the discontinuous functions and their derivatives on a front as we approach a curve of discontinuity from either side are finite. Such a discontinuity was first analyzed by Whitham in 1957 (see [34]), who called it shock-shock, meaning shock on a shock front. However, the theory of kinematical conservation laws (KCL) shows that a discontinuity of this type is geometric in nature and can arise on any propagating surface Ω_t, and hence it has been given a general name **kink**. In order to explain the existence of a kink and study its formation and propagation, we need the governing equations in the form a system of physically realistic conservation laws. In this paper we derive and analyze such conservation laws in a specially defined *ray coordinate system* and since they are derived purely on geometrical consideration and they have been called *kinematical conservation laws (KCL)*, [28]. When a discontinuous solution of the KCL system in the ray coordinates has a shock satisfying Rankine - Hugoniot conditions, the image of the shock in $\mathbb{R}^3$ is a kink.

Date: August 9, 2008.

2000 *Mathematics Subject Classification.* Primary 35L65, 35L67; Secondary 35L80.

Key words and phrases. kinematical conservation laws, ray theory, nonlinear waves, kinks, weakly hyperbolic system, finite difference scheme.

Before we start any discussion, we assume that all variables, both dependent and independent, used in this paper are nondimensional.

KCL governing the evolution of a moving curve Ω_t in two space dimensions (x_1, x_2) were first derived by Morton, Prasad and Ravindran [26] in 1992, and the kink (in this case, a point on Ω_t) phenomenon is well understood (see [28]-Section 3.3). We call this system of KCL as 2-D KCL which we describe in the next paragraph.

Consider a one parameter family of curves Ω_t in (x_1, x_2)-plane, where the subscript t is the parameter whose different values correspond to different positions of the moving curve. We assume that this family of curves has been obtained with the help of a ray velocity $\boldsymbol{\chi} = (\chi_1, \chi_2)$, which is a function of x_1, x_2, t and $\mathbf{n}$, where $\mathbf{n}$ is the unit normal to Ω_t. We further assume that motion of this curve Ω_t is isotropic so that we take the ray velocity $\boldsymbol{\chi}$ in the direction of $\mathbf{n}$ and write it as

$$\boldsymbol{\chi} = m\mathbf{n}, \tag{1.1}$$

where the scalar function m depends on $\mathbf{x}$ and t but is independent of $\mathbf{n}$. The ray equations

$$\frac{\mathrm{d}\mathbf{x}}{\mathrm{d}t} = m\mathbf{n}, \ \frac{\mathrm{d}\theta}{\mathrm{d}t} = -\left(-n_2\frac{\partial}{\partial x_1} + n_1\frac{\partial}{\partial x_2}\right)m, \tag{1.2}$$

where $\mathbf{n} = (n_1, n_2) = (\cos\theta, \sin\theta)$, are derived from Charpit's equations (or Hamilton's canonical equations) of an eikonal equation (see Section 2). The normal velocity m of Ω_t has been nondimensionlized with respect to a characteristic velocity (say the sound velocity a_0 in a uniform ambient medium in the case Ω_t is a wavefront in such a medium). Given a representation of the curve Ω_0 at the time $t = 0$ in the form $\mathbf{x} = \mathbf{x}_0(\xi)$, we determine the unit normal $\mathbf{n}_0(\xi)$ and then we solve the system (1.2) with these as initial values (this is a simplified view - the system (1.2) is usually under-determined as explained in the Section 3). Thus we get a representation of the curve Ω_t at time t in the form $\mathbf{x} = \mathbf{x}(\xi, t)$. We assume (for development of the theory) that this gives a mapping: $(\xi, t) \to (x_1, x_2)$ which is one to one. In this way we have introduced a ray coordinate system (ξ, t) such that $t =$ constant represents the curve Ω_t and $\xi =$ constant represents a ray. Then $m\mathrm{d}t$ is an element of distance along a ray, *i.e.,* m is the metric associated with the variable t. Let g be the metric associated with the variable ξ, then

$$\frac{1}{g}\frac{\partial}{\partial\xi} = -n_2\frac{\partial}{\partial x_1} + n_1\frac{\partial}{\partial x_2}. \tag{1.3}$$

Simple geometrical consideration gives (see [28]-Section 3.3 and also the Section 3 of this paper)

$$\mathrm{d}\mathbf{x} = (g\mathbf{u})\mathrm{d}\xi + (m\mathbf{n})\mathrm{d}t, \tag{1.4}$$

where $\mathbf{u}$ is the tangent vector to Ω_t, *i.e.,* $\mathbf{u} = (-n_2, n_1)$. Equating $(x_1)_{\xi t} = (x_1)_{t\xi}$ and $(x_2)_{\xi t} = (x_2)_{t\xi}$, we get the 2-D KCL

$$(gn_2)_t + (mn_1)_\xi = 0, \quad (gn_1)_t - (mn_2)_\xi = 0. \tag{1.5}$$

Using these KCL we can derive the Rankine-Hugoniot conditions (*i.e.,* the jump relations) relating the quantities on the two sides of a shock path in (ξ, t)-plane or a kink path in (x_1, x_2)-plane. The system (1.5) is under-determined since it contains only two equations in three variables θ, m and g. It is possible to close it in many ways. One possible way is to close it by a single conservation law

$$(gG^{-1}(m))_t = 0, \tag{1.6}$$

where G is a given function of m, see [4] for more details. For a weakly nonlinear wavefront ([28]-Chapter 6) in a polytropic gas, conservation of energy along a ray tube gives (with a suitable choice of ξ)

$$G(m) = (m-1)^{-2}e^{-2(m-1)}, \tag{1.7}$$

(see also the equation (3.6) in this article). Prasad and his collaborators have used this closure relation to solve many interesting problems and obtained many new results [5, 6, 25, 30]. KCL with (1.6) and (1.7) is a very interesting system. It is hyperbolic for $m > 1$ and has elliptic nature for $m < 1$.

The KCL for a surface evolving in three space dimensions (called 3-D KCL), a system of 6 conservation laws, were first obtained by Giles, Prasad and Ravindran [15]. Later on the analysis of 3-D KCL is completed by Arun and Prasad [2], which we discuss in the next section.

2. 3-D KCL of Giles, Prasad and Ravindran (1995)

Following the discussion in the last section consider a surface Ω in $\mathbb{R}^4$, $\Omega\colon \varphi(\mathbf{x}, t) = 0$ and let us assume that Ω is generated by a two parameter family of curves in $\mathbb{R}^4$, such that projection of these curves on $\mathbf{x}$-space are rays which are orthogonal to the successive position of the surface in $(\mathbf{x})$-space, $\Omega_t\colon \varphi(\mathbf{x}, t) = 0, t = \text{constant}$.

We introduce a ray coordinate system (ξ_1, ξ_2, t) in $\mathbf{x}$-space such that $t =$ constant represents the surface Ω_t at any time t, and ξ_1 and ξ_2 are surface coordinates on Ω_t, see [20]. The surface Ω_t in $\mathbf{x}$-space is now generated by a one parameter family of curves such that along each of these curves ξ_1 varies and the parameter ξ_2 is constant. Similarly Ω_t is generated by another one parameter family of curves along each of these ξ_2 varies and ξ_1 is constant. Through each point (ξ_1, ξ_2) of Ω_t there passes a ray orthogonal (in $\mathbf{x}$-space) to the successive positions of Ω_t, thus rays form a two parameter family as mentioned above. Given ξ_1, ξ_2 and t, we uniquely identify a point P in $\mathbf{x}$-space. For the development of theory, we assume that the mapping from (ξ_1, ξ_2, t)-space to (x_1, x_2, x_3)-space is one to one. On Ω_t let $\mathbf{u}$ and $\mathbf{v}$ be unit tangent vectors of the curves $\xi_2 =$ constant and $\xi_1 =$ constant respectively and $\mathbf{n}$ be unit normal to Ω_t. Then

$$\mathbf{n} = \frac{\mathbf{u} \times \mathbf{v}}{|\mathbf{u} \times \mathbf{v}|}. \tag{2.1}$$

Let an element of length along a curve ($\xi_2 =$ constant, $t =$ constant) be $g_1 \mathrm{d}\xi_1$ and that along a curve ($\xi_1 =$ constant, $t =$ constant) be $g_2 \mathrm{d}\xi_2$. The element of length along a ray ($\xi_1 =$ constant, $\xi_2 =$ constant) is $m\mathrm{d}t$, where m is the velocity of the surface Ω_t. The displacement $\mathrm{d}\mathbf{x}$ in $\mathbf{x}$-space due to increments $\mathrm{d}\xi_1$, $\mathrm{d}\xi_2$ and $\mathrm{d}t$ is given by (this is an extension of the result (1.4))

$$\mathrm{d}\mathbf{x} = (g_1\mathbf{u})\mathrm{d}\xi_1 + (g_2\mathbf{v})\mathrm{d}\xi_2 + (m\mathbf{n})\mathrm{d}t. \tag{2.2}$$

This gives

$$J := \frac{\partial(x_1, x_2, x_3)}{\partial(\xi_1, \xi_2, t)} = g_1 g_2 m \sin\chi, \quad 0 < \chi < \pi, \tag{2.3}$$

where $\chi(\xi_1, \xi_2, t)$ is the angle between the $\mathbf{u}$ and $\mathbf{v}$, *i.e.,*

$$\cos\chi = \langle \mathbf{u}, \mathbf{v} \rangle. \tag{2.4}$$

As explained after (3.6) in the next section, we shall like to choose $\sin\chi = |\mathbf{u} \times \mathbf{v}|$ which requires the restriction $0 < \chi < \pi$ on χ. For a smooth moving surface Ω_t, we equate $\mathbf{x}_{\xi_1 t} = \mathbf{x}_{t\xi_1}$ and $\mathbf{x}_{\xi_2 t} = \mathbf{x}_{t\xi_2}$, and get the 3-D KCL of Giles, Prasad and Ravindran [15],

$$(g_1\mathbf{u})_t - (m\mathbf{n})_{\xi_1} = 0, \tag{2.5}$$

$$(g_2\mathbf{v})_t - (m\mathbf{n})_{\xi_2} = 0. \tag{2.6}$$

We also equate $\mathbf{x}_{\xi_1\xi_2} = \mathbf{x}_{\xi_2\xi_1}$ and derive three more scalar equations contained in

$$(g_2\mathbf{v})_{\xi_1} - (g_1\mathbf{u})_{\xi_2} = 0. \tag{2.7}$$

Equations (2.5)-(2.7) are necessary and sufficient conditions for the integrability of the equation (2.2) (see [11], Section 1.9).

From the equations (2.5) and (2.6) we can show that $(g_2\mathbf{v})_{\xi_1} - (g_1\mathbf{u})_{\xi_2}$ does not depend on t. If any choice of coordinates ξ_1 and ξ_2 on Ω_0 implies that the condition (2.7) is satisfied at $t = 0$ then it follows that (2.7) is automatically satisfied. Thus, the 3-D KCL is a system of six scalar evolution equations (2.5) and (2.6). However, since $|\mathbf{u}| = 1$, $|\mathbf{v}| = 1$, there are 7 dependent variables in (2.5) and (2.6): two independent components of each of $\mathbf{u}$ and $\mathbf{v}$, the front velocity m of Ω_t, g_1 and g_2. Thus KCL is an under-determined system and can be closed only with the help of additional relations or equations, which would follow from the nature of the surface Ω_t and the dynamics of the medium in which it propagates.

We derive a few results from (2.5) and (2.6) without considering the closure equation (or equations) for m. The system (2.5) and (2.6) consists of equations which are conservation laws, so its weak solution may contain shocks which are surfaces in (ξ_1, ξ_2, t)-space. Across these **shock surfaces** m, g_1, g_2 and vectors $\mathbf{u}, \mathbf{v}$ and $\mathbf{n}$ will be discontinuous. Image of a shock surface into $\mathbf{x}$-space will be another surface, let us call it a **kink surface**, which will intersect Ω_t in a curve, say **kink curve** $\mathscr{K}_t$. Across this kink curve or simply the kink, the normal direction $\mathbf{n}$ of Ω_t will be discontinuous as shown in Figure 1. As time t evolves, $\mathscr{K}_t$ will generate the kink surface. A **shock front** (a phrase very commonly used in literature) is a curve in (ξ_1, ξ_2)-plane and its motion as t changes generates the shock surface in (ξ_1, ξ_2, t)-space. We assume that the mapping between (ξ_1, ξ_2, t)-space and (x_1, x_2, x_3)-space continues to be one to one even when a kink appears.

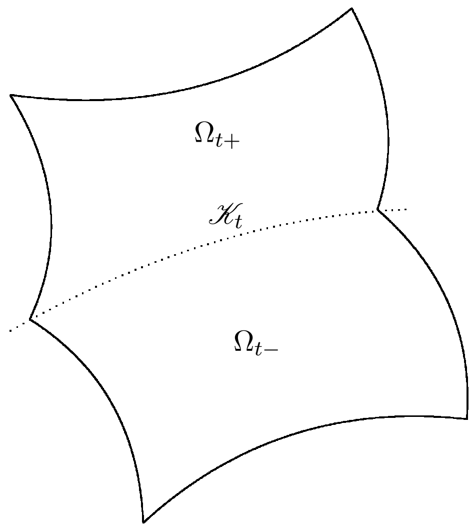

FIGURE 1. Kink curve $\mathscr{K}_t$ (shown with dotted lines) on $\Omega_t = \Omega_{t+} \cup \Omega_{t-}$

The distance $\mathrm{d}\mathbf{x}$ between two points $P(\mathbf{x})$ and $Q'(\mathbf{x} + \mathrm{d}\mathbf{x})$ on Ω_t and $\Omega_{t+\mathrm{d}t}$ respectively satisfies the relation (2.2), where (ξ_1, ξ_2, t) and $(\xi_1 + \mathrm{d}\xi_1, \xi_2 + \mathrm{d}\xi_2, t + \mathrm{d}t)$ are corresponding coordinates in (ξ_1, ξ_2, t)-space. If the points P and Q' are chosen to be points on the kink surface (see [28] for a two dimensional analog), then the conservation of $\mathrm{d}\mathbf{x}$ implies that the expression for $(\mathrm{d}\mathbf{x})_+$ on one side of the kink surface must be equal to the expression for $(\mathrm{d}\mathbf{x})_-$ on the other side. Denoting quantities on the two sides of the kink by subscripts + and -, we get

$$\begin{aligned} g_{1+}\mathrm{d}\xi_1\mathbf{u}_+ + g_{2+}\mathrm{d}\xi_2\mathbf{v}_+ + m_+\mathrm{d}t\mathbf{n}_+ \\ = g_{1-}\mathrm{d}\xi_1\mathbf{u}_- + g_{2-}\mathrm{d}\xi_2\mathbf{v}_- + m_-\mathrm{d}t\mathbf{n}_-. \end{aligned} \tag{2.8}$$

We take the direction of the line element PQ' such that its projection on (ξ_1, ξ_2)-plane is in the direction of the normal to the shock curve in (ξ_1, ξ_2)-plane, then the differentials are further restricted. Let the unit normal of this shock curve be (E_1, E_2) and let K be its velocity of propagation in this plane, then the differentials in (2.8) satisfy $\frac{\mathrm{d}\xi_1}{\mathrm{d}t} = E_1K$ and $\frac{\mathrm{d}\xi_2}{\mathrm{d}t} = E_2K$, and (2.8) now becomes

$$\begin{aligned} (g_{1+}E_1\mathbf{u}_+ + g_{2+}E_2\mathbf{v}_+)K + m_+\mathbf{n}_+ \\ = (g_{1-}E_1\mathbf{u}_- + g_{2-}E_2\mathbf{v}_-)K + m_-\mathbf{n}_-. \end{aligned} \tag{2.9}$$

Thus (2.9) is a condition for the conservation of distance (in three independent directions in $\mathbf{x}$*-space) across a kink surface when a point moves along the normal to the shock curve in* (ξ_1, ξ_2)*-plane.*

Using the usual method for the derivation of jump conditions across a shock, we deduce from the conservation laws (2.5) and (2.6)

$$K[g_1\mathbf{u}] + E_1[m\mathbf{n}] = 0, \quad K[g_2\mathbf{v}] + E_2[m\mathbf{n}] = 0, \tag{2.10}$$

where a jump $[f]$ of a quantity f is defined by

$$[f] = f_+ - f_-. \tag{2.11}$$

Multiplying the first relation in (2.10) by E_1 and the second relation by E_2, adding and using $E_1^2 + E_2^2 = 1$, we get

$$E_1K[g_1\mathbf{u}] + E_2K[g_2\mathbf{v}] + [m\mathbf{n}] = 0, \tag{2.12}$$

which is the same as (2.9). Thus we have proved the following theorem, see also [15].

Theorem 2.1. *The six jump relations (2.10) imply conservation of distance in* x_1, x_2 *and* x_3 *directions (and hence in any arbitrary direction in* $\mathbf{x}$*-space) in the sense that the expressions for a vector displacement* $(\mathrm{d}\mathbf{x})_{\mathscr{K}_t}$ *of a point of the kink line* $\mathscr{K}_t$ *in an infinitesimal time interval dt, when computed in terms of variables on the two sides of a kink surface, have the same value. This displacement of the point is assumed to take place on the kink surface and that of its image in* (ξ_1, ξ_2, t)*-space takes place on the shock surface such that the corresponding displacement in* (ξ_1, ξ_2)*-plane is in direction* $\frac{d}{dt}(\xi_1, \xi_2) = (E_1, E_2)K$ *so that the displacement remains on the shock front.*

This theorem assures that the 3-D KCL are physically realistic. Consider a point P on a kink line $\mathscr{K}_t$ on Ω_t and two straight lines T_- and T_+ orthogonal to the kink line at P and lying in the tangent planes at P to Ω_{t-} and Ω_{t+} on the two sides of $\mathscr{K}_t$. Let N_- and N_+ be normals to the two tangent planes at P. Then the four lines T_+, N_+, N_- and T_-, being orthogonal to the kink line at P, are coplanar. A kink phenomenon is basically two dimensional. Locally, the two sides Ω_{t-} and Ω_{t+} of Ω_t can be regarded to be planes separated by a straight kink line. Hence the evolution of the kink phenomena can be viewed locally in a plane which intersects the planes Ω_{t-}, Ω_{t+} and $\mathscr{K}_t$ orthogonally as shown in the Figure 3.3.4 of [28].

We state an important result which will be very useful in proving many properties of the KCL and in setting up the Cauchy data on Ω_0. *Let* $P_0(\mathbf{x}_0)$ *be a given point on* Ω_t *at any time t. Then there exist two one parameter families of smooth curves on* Ω_t *such that the unit vectors* $\mathbf{u}_0$ *and* $\mathbf{v}_0$ *along the members of the two families through the chosen point* P_0 *can have any two arbitrary directions and the metrics* g_{10} *and* g_{20} *at this point can have any two positive values.*

3. Energy transport equation from a WNLRT for a polytropic gas and the complete set of equations

In this section we shall derive a closure relation in a conservation form for the 3D-KCL so that we get a completely determined system of conservation laws. Let the mass density, fluid velocity, gas pressure and local sound velocity in a polytropic gas [12] be denoted by $\varrho, \mathbf{q}, p$ and a. Consider a member Ω_t of a one parameter family of curved nonlinear wavefronts in a small amplitude wave moving with the characteristic velocity $\mathbf{q} + a$ and running into the gas in a uniform state and at rest ($\varrho_0 =$ constant, $\mathbf{q} = 0$ and $p_0 =$ constant, [28]-Sections 1.8 and 6.1). Then a perturbation in the state of the gas on Ω_t can be expressed in terms of an amplitude w and is given by

$$\varrho - \varrho_0 = \left(\frac{\varrho_0}{a_0}\right) w, \ \ \mathbf{q} = \mathbf{n}w, \ \ p - p_0 = \varrho_0 a_0 w, \tag{3.1}$$

where a_0 is the sound velocity in the undisturbed medium $= \sqrt{\gamma p_0/\varrho_0}$ and w is a quantity of small order, say $\mathcal{O}(\epsilon)$. Let us remind, what we stated in the Section 1, that all dependent variables are dimensional in this (and only in this) paragraph. Note that w here has the dimension of velocity. The amplitude w is related to the non-dimensional normal velocity m of Ω_t by

$$m = 1 + \frac{\gamma+1}{2}\frac{w}{a_0}. \tag{3.2}$$

The operator $\frac{\mathrm{d}}{\mathrm{d}t} = \frac{\partial}{\partial t} + m\langle \mathbf{n}, \nabla\rangle$ in space-time becomes simply the partial derivative $\frac{\partial}{\partial t}$ in the ray coordinate system (ξ_1, ξ_2, t). Hence the energy transport equation of the WNLRT ([28]-equation (6.1.3)) in non-dimensional coordinates becomes

$$m_t = (m-1)\mathit{\Omega} = -\frac{1}{2}(m-1)\langle \nabla, \mathbf{n}\rangle, \tag{3.3}$$

where the italic symbol $\mathit{\Omega}$ is the mean curvature of the wavefront Ω_t. Ray tube area A for any ray system ([34]-pages 244, 280, [28]-relation (2.2.23)) is related to the mean curvature $\mathit{\Omega}$ (we write here in non-dimensional variables) by

$$\frac{1}{A}\frac{\partial A}{\partial l} = -2\mathit{\Omega}, \ \ \frac{\partial}{\partial l} \text{ in ray coordinates,} \tag{3.4}$$

where l is the arc length along a ray. In non-dimensional variables we have $\mathrm{d}l = m\mathrm{d}t$. From (3.3) and (3.4) we get

$$\frac{2m_t}{m-1} = -\frac{1}{mA}A_t. \tag{3.5}$$

This leads to a conservation law, which we accept to be the required one,

$$\left\{(m-1)^2 e^{2(m-1)} A\right\}_t = 0. \tag{3.6}$$

We note that contrary to the result for the energy transport equation in the form $\left\{(m-1)^2 A\right\}_t = 0$ in a linear ray tube, we now have an addition factor $e^{2(m-1)}$ coming from nonlinear stretching of the rays.

Integration gives $(m-1)^2 e^{2(m-1)} A = F(\xi_1, \xi_2)$, where F is an arbitrary function of ξ_1 and ξ_2. The ray tube area A is given by $A = g_1 g_2 \sin\chi$, where χ is defined by (2.4). In order that A is positive, we need to choose $0 < \chi < \pi$. Now the energy conservation equation becomes

$$\left\{(m-1)^2 e^{2(m-1)} g_1 g_2 \sin\chi\right\}_t = 0. \tag{3.7}$$

The complete set of conservation laws for the weakly nonlinear ray theory (WNLRT) for a polytropic gas are: the six equations in (2.5)-(2.6) and the equation (3.7). The equations (2.7) need to be satisfied at any fixed t, say at $t = 0$. Once we have a solution of this system in

(ξ_1, ξ_2, t)-space, the results can be mapped into the $\mathbf{x}$-space by the relation (2.2), which implies the equation (4.2) given below. This would give successive positions of a wavefront Ω_t.

4. Some properties of the system of equations of 3-D WNLRT and formulation of the ray coordinates for a particular surface

Our main aim in this paper is to get some interesting results from numerical solution of the system of equations of 3-D WNLRT and to show the efficiency of numerical schemes for this complex system. For this purpose, the results of the last two sections are sufficient. However, in order to get a deeper understanding of the WNLRT, we need to know some important properties of the system after considerable amount of calculations and analysis. Hence we simply quote these properties from the reference [2].

We state the first result in the form of a theorem:

Theorem 4.1. *For a given smooth function m of $\mathbf{x}$ and t, the ray equations*

$$\frac{d\mathbf{x}}{dt} = m\mathbf{n}, \quad |\mathbf{n}| = 1, \tag{4.1}$$

$$\frac{d\mathbf{n}}{dt} = -\mathbf{L}m := -\left(\nabla - \mathbf{n}\langle \mathbf{n}, \nabla\rangle\right) m. \tag{4.2}$$

are equivalent to the KCL as long as their solutions are smooth.

This is a very interesting result since ray equations follow from the theory of an eikonal equation (a partial differential equation for φ in $\mathbb{R}^4$, where $\Omega\colon \varphi(\mathbf{x}, t) = 0$) whereas KCL is a purely geometric result.

The system of 7 conservation laws (2.5)-(2.6) and the equation (3.7) are quite complex. After considerable algebraic calculations, we can derive a system of 7 differential equations in the usual vector notation for the vector $U = (u_1, u_2, v_1, v_2, m, g_1, g_2)^T$ as

$$AU_t + B^{(1)}U_{\xi_1} + B^{(2)}U_{\xi_2} = 0, \tag{4.3}$$

where u_1, u_2 and v_1, v_2 are the first two components of the unit vectors $\mathbf{u}$ and $\mathbf{v}$ respectively. The expressions for the matrices A, $B^{(1)}$ and $B^{(2)}$ are given in [2].

We can use also the above differential form of the KCL to deduce the ray equations. However, the most important use of (4.3) would be derivation of the eigenvalues and eigenfunctions of the equations of WNLRT, which we state in the form of another theorem:

Theorem 4.2. *The system (4.3) has 7 eigenvalues $\lambda_1, \lambda_2 (= -\lambda_1), \lambda_3 = \lambda_4 = \ldots = \lambda_7 = 0$, where λ_1 and λ_2 are real for $m > 1$ and purely imaginary for $m < 1$. Further, the dimension of the eigenspace corresponding to the multiple eigenvalue 0 is 4.*

Since it has not been possible so far to factorize the characteristic equation for the eigenvalue λ of the system (4.3), namely $\det\left(-\lambda A + e_1 B^{(1)} + e_2 B^{(2)}\right) = 0$, this result has been derived indirectly in [2]. Firstly, due to the result mentioned at the end of the Section 2, we can first choose a fixed point P_0 on Ω_t in (x_1, x_2, x_3)-space. At this point, we take the $\xi_2 =$ constant and $\xi_1 =$ constant curves to be orthogonal, so that the unit tangent vectors in $(\mathbf{u}, \mathbf{v})_{P_0} = (\mathbf{u}', \mathbf{v}')$ are orthogonal. The corresponding characteristic matrix can now be factorized and we can get the eigenvalues. Two eigenvalues turn out to be nonzero and distinct, and a zero eigenvalue with multiplicity 5 but the dimension of the eigenspace corresponding to this multiple eigenvalue is only 4. Now we can make a linear transformation from the orthogonal vectors $(\mathbf{u}', \mathbf{v}')$ to a general nonorthogonal vectors $(\mathbf{u}, \mathbf{v})_{P_0}$ in the tangent plane to Ω_t at P_0 and get the eigenvalues for an arbitrary coordinate system at this point. This procedure leads to the result stated in the above theorem, see [2] for more details.

The use of the transformation procedure mentioned in the above theorem has another deep result highlighting the relation between the eigenvalues appearing in a special formulation of a part of the ray equations, namely (4.2) and the KCL, [2]. We stop this discussion here as it takes us away from the main aim of this paper.

There is an extensive discussion of the above results in [2], which puts the theory of 3-D KCL on a strong foundation. In this paper we use 3-D KCL to discuss evolution of a surface Ω_t in three space dimensions and formation and propagation of curves of singularities on Ω_t. However, there is now a special challenge since the Theorem 4.2 shows that the eigenspace of the eigenvalue 0 is not complete so that WNLRT equations are weakly hyperbolic. Theory of weakly hyperbolic system is an active area of research, [13, 21, 23, 24, 31, 33] since the last 15 years but it is very much incomplete. Appearance of δ waves and δ shocks in the solution of such systems make the numerical approximation of weakly hyperbolic system very complex, see [14]. The main aim of this paper is not to do an intensive computation on the problem of three dimensional nonlinear wavefronts but to test the numerical efficacy of the 3-D KCL theory using 3-D WNLRT equations.

Now we pass on to the formulation of the ray coordinates on a given surface and show how to set up the initial value problem for the equations of WNLRT. Let the initial position of a weakly nonlinear wavefront Ω_t be given as

$$\Omega_0\colon x_3 = f(x_1, x_2). \tag{4.4}$$

On Ω_0 we choose

$$\xi_1 = x_1,\ \xi_2 = x_2, \tag{4.5}$$

then

$$\Omega_0\colon x_{10} = \xi_1,\ x_{20} = \xi_2,\ x_{30} = f(\xi_1, \xi_2) \tag{4.6}$$

and

$$g_{10} = \sqrt{1 + f_{\xi_1}^2}, \quad \mathbf{u}_0 = \frac{(1, 0, f_{\xi_1})}{\sqrt{1 + f_{\xi_1}^2}}, \tag{4.7}$$

$$g_{20} = \sqrt{1 + f_{\xi_2}^2}, \quad \mathbf{v}_0 = \frac{(0, 1, f_{\xi_2})}{\sqrt{1 + f_{\xi_2}^2}}. \tag{4.8}$$

We can easily check that (2.7) is satisfied on Ω_0. The unit normal $\mathbf{n}_0$ on Ω_0 is

$$\mathbf{n}_0 = -\frac{(f_{\xi_1}, f_{\xi_2}, -1)}{\sqrt{1 + f_{\xi_1}^2 + f_{\xi_2}^2}} \tag{4.9}$$

in which the sign is so chosen such that $(\mathbf{u}, \mathbf{v}, \mathbf{n})$ form a right handed system. Let the distribution of the front velocity be given by

$$m = m_0(\xi_1, \xi_2). \tag{4.10}$$

We have now completed formulation of the initial data for the KCL (2.5) and (2.6), and the energy transport equation (3.7).

The problem is to find solution of the system (2.5), (2.6) and (3.7) satisfying the initial data given by (4.7),(4.8) and (4.10). Having solved these equations, we can get Ω_t by solving the first part of the ray equations (4.1) at least numerically for a number of values of ξ_1 and ξ_2. In the next section we approximate (2.5), (2.6) and (3.7) using both the first order staggered Lax-Friedrichs scheme and the second order Nessyahu-Tadmor scheme.

5. Numerical Approximation

Due to the fact that we have an incomplete set of eigenvectors the system (2.5)-(2.6), (3.7) is weakly hyperbolic. Thus it is not well-posed in the strong hyperbolic sense and likely to be more sensitive than regular hyperbolic systems. This is also reflected in difficulties with obtaining a stable numerical approximation as we will see in Section 6, cf. second test case. The existence of the solution to weakly hyperbolic systems is an open problem in general. Numerical as well as theoretical analysis indicates that the solution does not belongs to BV spaces and is only measure valued. Clearly, due to the fact that we have a multiple eigenvalue $\lambda = 0$ typically δ function appears in the corresponding fields, which are linearly degenerate in our case. In addition they interact with the genuinely nonlinear field, that typically obtains shock. This yields the product of δ function with Heaviside distribution, which can be defined using measure theory. In literature one can find several publications, where such solutions have been studied for certain weakly hyperbolic systems, see [7, 9, 10, 13, 14, 16, 31, 32, 33] and the references therein; see also [8, 22] for numerical approximations of certain weakly hyperbolic systems. In our subsequent paper we want to study theoretically simplified model problems corresponding to the 3D-KCL system. For example, our goals will be construction of a solution to the Riemann problem or analytical results on existence of measure-valued solution. The aim of this section is to present a numerical solution of the KCL (2.5)-(2.6) and (3.7) using simple but robust central schemes. In particular we work with the first order staggered Lax-Friedrichs scheme [19] and the second order Nessyahu-Tadmor scheme [27].

Note that the KCL (2.5)-(2.6) and the energy transport equation (3.7) of WNLRT for the variable $U = (u_1, u_2, v_1, v_2, m, g_1, g_2)^T$ can be written as a system of conservation laws

$$(H(U))_t + (F_1(U))_{\xi_1} + (F_2(U))_{\xi_2} = 0, \tag{5.1}$$

where

$$\begin{aligned}
H(U) &= \Big(g_1u_1, g_1u_2, g_1u_3, g_2v_1, g_2v_2, g_2v_3, (m-1)^2 e^{2(m-1)} g_1 g_2 \sin\chi\Big)^T,\\
F_1(U) &= (mn_1, mn_2, mn_3, 0, 0, 0, 0)^T,\\
F_2(U) &= (0, 0, 0, mn_1, mn_2, mn_3, 0)^T.
\end{aligned}$$

We briefly review the staggered Lax-Friedrichs scheme and the Nessyahu-Tadmor scheme for the system of conservation laws (5.1), see [1, 17, 18, 19, 27] for more details.

We denote the mesh points by ${\xi_1}_i = i\Delta\xi_1, {\xi_2}_j = j\Delta\xi_2, t_n = n\Delta t, i, j, \in \mathbb{Z}, n \in \mathbb{N}$. Let U^n_{ij} be an approximation to $U(i\Delta\xi_1, j\Delta\xi_2, n\Delta t)$. Note that the staggered schemes make use of two types of grids. At odd time steps we use the original mesh cells,

$$C_{i,j} = \left[{\xi_1}_{i-\frac{1}{2}}, {\xi_1}_{i+\frac{1}{2}}\right] \times \left[{\xi_2}_{j-\frac{1}{2}}, {\xi_2}_{j+\frac{1}{2}}\right]$$

and at even time steps the so-called dual or staggered grid is used

$$C_{i+\frac{1}{2},j+\frac{1}{2}} = \left[{\xi_1}_i, {\xi_1}_{i+1}\right] \times \left[{\xi_2}_j, {\xi_2}_{j+1}\right],$$

see Figure 2.

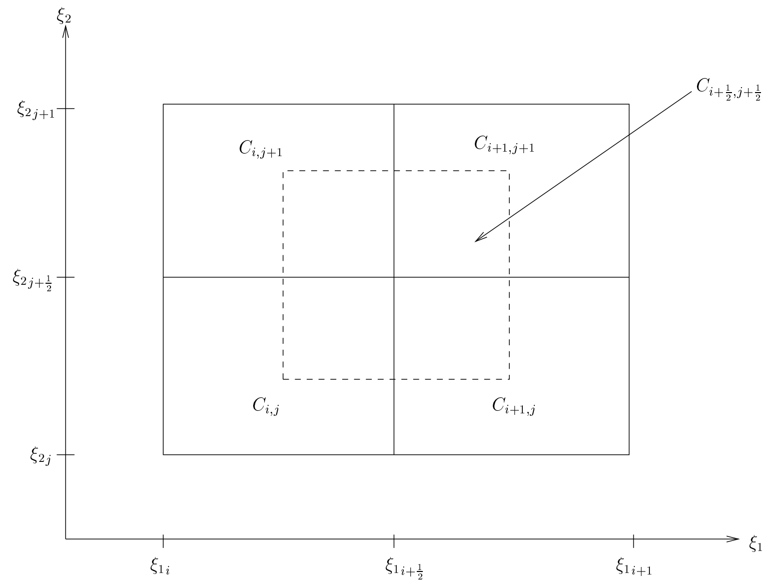

FIGURE 2. Computational stencil: the original grid is depicted by solid lines and a dual grid is denoted by dotted lines.

5.1. **Lax-Friedrichs Scheme.** In the staggered version the Lax-Friedrichs method produces the cell average at time t^{n+1} as given by

$$\begin{aligned} H(U^{n+1}_{i+\frac{1}{2},j+\frac{1}{2}}) =& \frac{1}{4}\left\{H(U^n_{i,j}) + H(U^n_{i+1,j}) + H(U^n_{i,j+1}) + H(U^n_{i+1,j+1})\right\} \\ & - \frac{\lambda_1}{2}\left\{F_1(U^n_{i+1,j}) - F_1(U^n_{i,j}) + F_1(U^n_{i+1,j+1}) - F_1(U^n_{i,j+1})\right\} \\ & - \frac{\lambda_2}{2}\left\{F_2(U^n_{i,j+1}) - F_2(U^n_{i,j}) + F_2(U^n_{i+1,j+1}) - F_2(U^n_{i+1,j})\right\}, \end{aligned} \tag{5.2}$$

where $\lambda_i = \Delta t/\Delta\xi_i, i = 1,2$ are the mesh ratios. The cell average $H(U^{n+1}_{i,j})$ at the original mesh is obtained by interpolating the staggered cell averages

$$H(U^{n+1}_{i,j}) = \frac{1}{4}\left\{H(U^{n+1}_{i+\frac{1}{2},j+\frac{1}{2}}) + H(U^{n+1}_{i-\frac{1}{2},j+\frac{1}{2}}) + H(U^{n+1}_{i-\frac{1}{2},j-\frac{1}{2}}) + H(U^{n+1}_{i+\frac{1}{2},j-\frac{1}{2}})\right\}. \tag{5.3}$$

5.2. **Nessyahu-Tadmor Scheme.** The Nessyahu-Tadmor scheme [1, 17, 18, 27] is a second order TVD extension of the Lax-Friedrichs scheme. It is a two step predictor-corrector method. In the predictor step we compute the value of the conserved variable at half time step

$$H(U^{n+\frac{1}{2}}_{i,j}) = H(U^n_{i,j}) - \frac{\lambda_1}{2}F_1(U^n_{i,j})' - \frac{\lambda_2}{2}F_2(U^n_{i,j})^{\backprime}, \tag{5.4}$$

where $(\cdot)' \approx \Delta\xi_1\partial_{\xi_1}(\cdot)$ and $(\cdot)^{\backprime} \approx \Delta\xi_2\partial_{\xi_2}(\cdot)$ are suitable finite difference operators. For example, the slopes can be approximated using the minmod limiter in the following way

$$\begin{aligned} (F_{1}{}^n_{i,j})' &= MM\left\{\theta\left(F_{1}{}^n_{i+1,j} - F_{1}{}^n_{i,j}\right), \frac{1}{2}\left(F_{1}{}^n_{i+1,j} - F_{1}{}^n_{i-1,j}\right), \theta\left(F_{1}{}^n_{i,j} - F_{1}{}^n_{i-1,j}\right)\right\}, \\ (F_{2}{}^n_{i,j})^{\backprime} &= MM\left\{\theta\left(F_{2}{}^n_{i,j+1} - F_{2}{}^n_{i,j}\right), \frac{1}{2}\left(F_{2}{}^n_{i,j+1} - F_{2}{}^n_{i,j-1}\right), \theta\left(F_{2}{}^n_{i,j} - F_{2}{}^n_{i,j-1}\right)\right\}. \end{aligned}$$

We have denoted ${F_k}^n_{i,j} = F_k(U^n_{i,j})$, for $k = 1, 2$, the parameter θ takes values in $[1, 2]$. The nonlinear minmod function is defined by

$$MM\{v_1, v_2, \cdots\} = \begin{cases} \min_p\{v_p\} & \text{if } v_p > 0\ \forall p, \\ \max_p\{v_p\} & \text{if } v_p < 0\ \forall p, \\ 0 & \text{otherwise.} \end{cases}$$

In the corrector step of the Nessyahu-Tadmor scheme the staggered average $H(U^{n+1}_{i+\frac{1}{2},j+\frac{1}{2}})$ at time t^{n+1} is updated as follows

$$\begin{aligned} H(U^{n+1}_{i+\frac{1}{2},j+\frac{1}{2}}) =& H(U^n_{i+\frac{1}{2},j+\frac{1}{2}}) \\ & - \frac{\lambda_1}{2}\left\{F_1(U^{n+\frac{1}{2}}_{i+1,j}) - F_1(U^{n+\frac{1}{2}}_{i,j}) + F_1(U^{n+\frac{1}{2}}_{i+1,j+1}) - F_1(U^{n+\frac{1}{2}}_{i,j+1})\right\} \\ & - \frac{\lambda_2}{2}\left\{F_2(U^{n+\frac{1}{2}}_{i,j+1}) - F_2(U^{n+\frac{1}{2}}_{i,j}) + F_2(U^{n+\frac{1}{2}}_{i+1,j+1}) - F_2(U^{n+\frac{1}{2}}_{i+1,j})\right\}. \end{aligned} \tag{5.5}$$

Note that we use a piecewise linear reconstruction of the conserved variable $H(U^n_{i,j})$ on the original grid

$$H\left(U(\xi_1, \xi_2, t^n)\right) = H(U^n_{i,j}) + \frac{(\xi_1 - \xi_{1i})}{\Delta\xi_1} H(U^n_{i,j})' + \frac{(\xi_2 - \xi_{2j})}{\Delta\xi_2} H(U^n_{i,j})^{\backprime}, \tag{5.6}$$

where the slopes are computed as

$$\begin{aligned} (H^n_{i,j})' &= MM\left\{\theta\left(H^n_{i+1,j} - H^n_{i,j}\right), \frac{1}{2}\left(H^n_{i+1,j} - H^n_{i-1,j}\right), \theta\left(H^n_{i,j} - H^n_{i-1,j}\right)\right\}, \\ (H^n_{i,j})^{\backprime} &= MM\left\{\theta\left(H^n_{i,j+1} - H^n_{i,j}\right), \frac{1}{2}\left(H^n_{i,j+1} - H^n_{i,j-1}\right), \theta\left(H^n_{i,j} - H^n_{i,j-1}\right)\right\}. \end{aligned}$$

Here $H^n_{i,j}$ is a shortcut for $H(U^n_{i,j})$. Now the staggered average $H(U^n_{i+\frac{1}{2},i+\frac{1}{2}})$ at the time level t^n can be obtained by averaging the linear functions (5.6)

$$\begin{aligned} H(U^n_{i+\frac{1}{2},j+\frac{1}{2}}) =& \frac{1}{4}\left\{H(U^n_{i,j}) + H(U^n_{i+1,j}) + H(U^n_{i+1,j+1}) + H(U^n_{i,j+1})\right\} \\ & + \frac{1}{16}\left\{H(U^n_{i,j})' - H(U^n_{i+1,j})' - H(U^n_{i+1,j+1})' + H(U^n_{i,j+1})'\right\} \\ & + \frac{1}{16}\left\{H(U^n_{i,j})^{\backprime} + H(U^n_{i+1,j})^{\backprime} - H(U^n_{i+1,j+1})^{\backprime} - H(U^n_{i,j+1})^{\backprime}\right\}. \end{aligned} \tag{5.7}$$

Finally the cell average $H(U^{n+1}_{i,j})$ is obtained by linear interpolation of the staggered averages $H(U^n_{i+\frac{1}{2},j+\frac{1}{2}})$ and by averaging, [18]

$$\begin{aligned} H^{n+1}_{i,j} =& \frac{1}{4}\left\{H^{n+1}_{i+\frac{1}{2},j+\frac{1}{2}} + H^{n+1}_{i-\frac{1}{2},j+\frac{1}{2}} + H^{n+1}_{i-\frac{1}{2},j-\frac{1}{2}} + H^{n+1}_{i+\frac{1}{2},j-\frac{1}{2}}\right\} \\ & + \frac{1}{16}\left\{\left(H^{n+1}_{i-\frac{1}{2},j-\frac{1}{2}}\right)' - \left(H^{n+1}_{i+\frac{1}{2},j-\frac{1}{2}}\right)' + \left(H^{n+1}_{i-\frac{1}{2},j+\frac{1}{2}}\right)' - \left(H^{n+1}_{i+\frac{1}{2},j+\frac{1}{2}}\right)'\right\} \\ & + \frac{1}{16}\left\{\left(H^{n+1}_{i-\frac{1}{2},j-\frac{1}{2}}\right)^{\backprime} - \left(H^{n+1}_{i-\frac{1}{2},j+\frac{1}{2}}\right)^{\backprime} + \left(H^{n+1}_{i+\frac{1}{2},j-\frac{1}{2}}\right)^{\backprime} - \left(H^{n+1}_{i+\frac{1}{2},j+\frac{1}{2}}\right)^{\backprime}\right\}. \end{aligned} \tag{5.8}$$

Notice that both the Lax-Friedrichs scheme (5.2) and the Nessyahu-Tadmor scheme (5.5) give the update for $H(U^{n+1}_{i,j})$. In order to get the values of the variables $m, g_1, g_2, \mathbf{u}$ and $\mathbf{v}$ we need to employ an appropriate nonlinear solver. In our numerical experiments a fixed point iteration has been used in (3.7). After computing the normal vector $\mathbf{n}$ from (2.1) we integrate the ray equations (4.1) to determine the wavefront at new time t^{n+1}. Here we have used the compound trapezoidal rule for the numerical integration in time.

6. Numerical experiments

In order to demonstrate applicability of the 3-D KCL for modelling of time evolution of nonlinear wavefronts we present in this section two illustrating examples. Interesting phenomena such as a kink line and a point singularity can be noticed in the physical $(x_1, x_2, x_3)-$space. On the other hand the resulting functions in the ray coordinates still remain single valued.

In the **first test case** the initial wavefront Ω_0 has the shape of a Gaussian pulse

$$\Omega_0\colon x_3 = e^{-(x_1^2+x_2^2)} \equiv f(x_1, x_2). \tag{6.1}$$

On Ω_0 the ray coordinates ξ_1 and ξ_2 can be chosen to be

$$\xi_1 = x_1, \quad \xi_2 = x_2. \tag{6.2}$$

Using (4.7)-(4.8) the initial values for the metrics g_1, g_2 and the vectors $\mathbf{u}$ and $\mathbf{v}$ can be obtained to be

$$g_{10} = \left(1 + f_{\xi_1}^2\right)^{1/2}, \quad g_{20} = \left(1 + f_{\xi_2}^2\right)^{1/2}. \tag{6.3}$$

$$\mathbf{u}_0 = \frac{1}{g_1}\left(1, 0, f_{\xi_1}\right), \quad \mathbf{v}_0 = \frac{1}{g_2}\left(0, 1, f_{\xi_2}\right). \tag{6.4}$$

The initial value of m is set to $m_0 = 1.2$. The computational domain is taken to be the square $[-5, 5] \times [-5, 5]$ and time evolution of nonlinear wavefront is calculated up to the final time $t = 2.5$. We have used a grid with 200×200 cells. In order to keep the method stable the following CFL stability condition has been used

$$\frac{\Delta t}{h} \max(\rho_1, \rho_2) \leq \text{CFL},$$

where $h = \Delta\xi_1 = \Delta\xi_2$ is a mesh step and ρ_1, ρ_2 are respectively maximum generalized eigenvalues of the Jacobian matrices $B^{(1)}$ and $B^{(2)}$ with respect to A, cf. (4.3). Here we have taken the CFL number 0.45. For the generalized limiter defined in the Subsection 5.2 the parameter θ was set to 2.

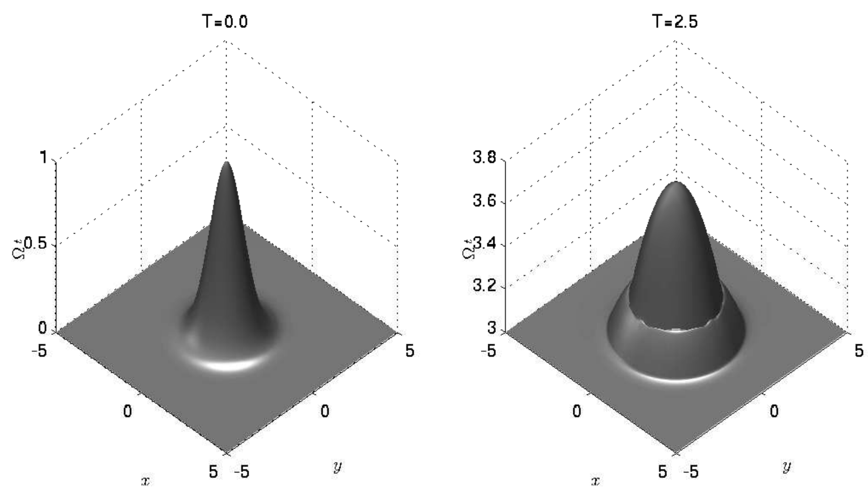

Figure 3. The nonlinear wavefront Ω_t starting initially in the shape of a Gaussian elevation.

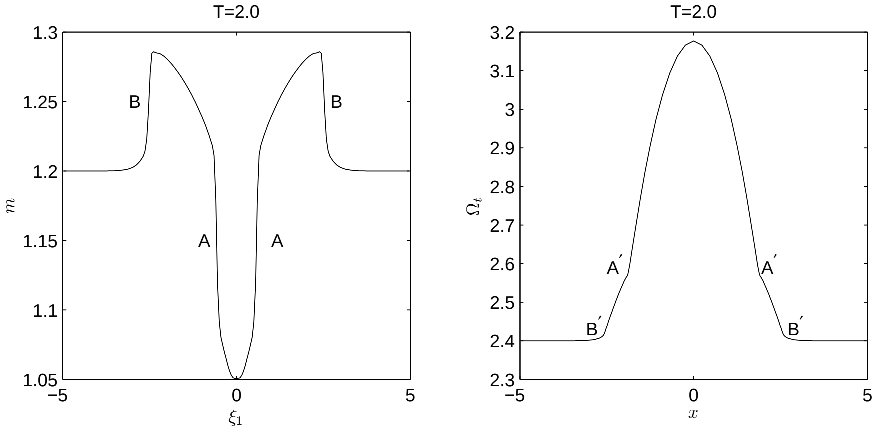

FIGURE 4. The kink lines A' and B' in (x_1, x_2, x_3)-space are images of shocks A and B in the ray coordinate system.

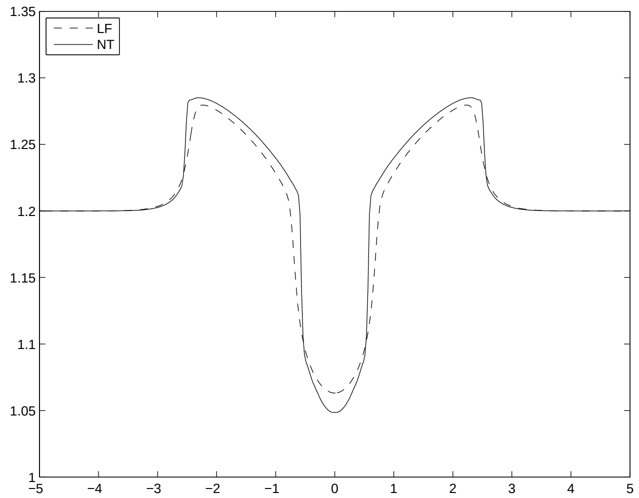

FIGURE 5. Time evolution of m at the cross-section $\xi_2 = 0$ for $t = 2.5$ obtained by the Lax-Friedrichs and the Nessyahu-Tadmor methods.

In Figure 3 we show the surface plot of the initial wavefront Ω_0 and the wavefront Ω_t at time $t = 2.5$. The wavefront at $t = 2.5$ has moved up in the x_3-direction and has spread over a larger area in (x_1, x_2)-plane and its height has decreased. The two kink circles are clearly seen as sharp lines, one at the base $x_3 = 3$ and another above it. As already mentioned in the Section 5 the position of Ω_t has been obtained by numerical integration of the ray equations (4.1).

In Figure 4 we plot the graph of $m = m(\xi_1)$ in $\xi_2 = 0$ plane and the shape of Ω_t with respect to x_1 in the cross-section $x_2 = 0$ at time $t = 2.0$. From the $(m - \xi)$ graph we find two shocks A and B (which would become shock circles in (m, ξ_1, ξ_2)-space). These shocks map onto two kinks A' and B' (or kink circles in (x_1, x_2, x_3)-space). For a detailed discussion on the formation and propagation of kinks in a two dimensional problem and resolution of a caustic due to nonlinearity the reader is referred to [5, 25, 28, 30].

Next we present the time evolution of the normal velocity m and metrics g_1, g_2 with respect to ξ_1 (in $\xi_2 = 0$ plane) in Figures 5, 6, 7 and 8. In Figure 5 both results obtained by the Lax-Friedrichs

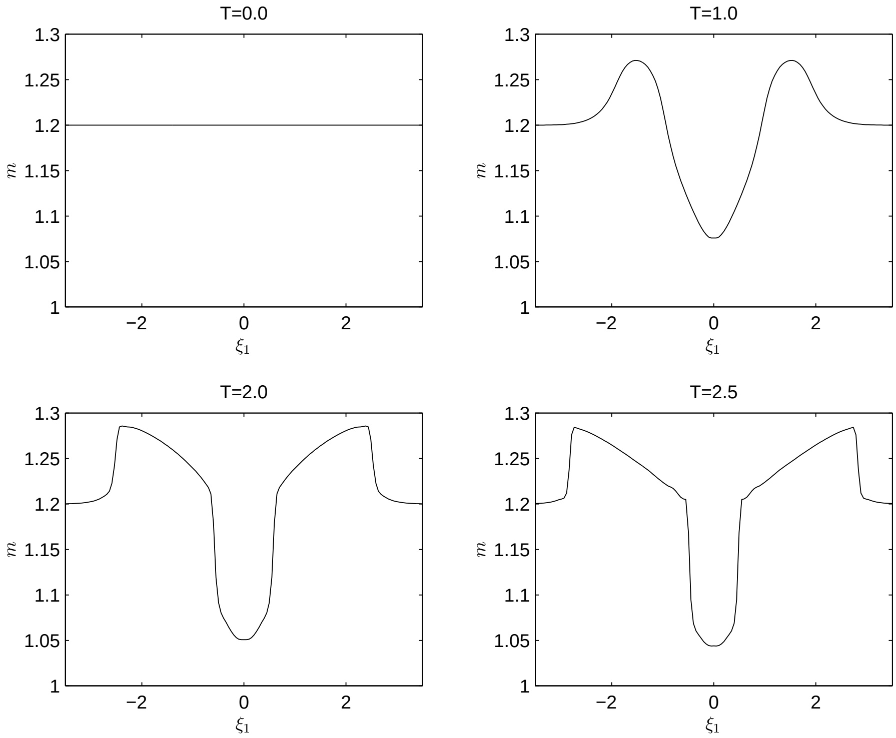

FIGURE 6. Time evolution of m at the cross-section $\xi_2 = 0$.

scheme and by the Nessyahu-Tadmor are plotted. As expected the second order Nessyahu-Tadmor resolves shocks more sharply. In the following pictures we just present the results obtained by the second order Nessyahu-Tadmor scheme.

From the plots of m, g_1 and g_2 we find that when m decreases (increases) the value of g_1 increases (decreases) but the value of g_2 always keeps on increasing in $\xi_2 = 0$ plane. However, all these changes remain consistent with the conservation law (3.7), which states that $(m-1)^2 e^{2(m-1)} g_1 g_2 \sin\chi =$ const. We have not given the graph of χ. From the results of m and g_1 it is clear that the shocks arise between $t = 1$ and $t = 2$.

Now we present the results in physical space (x_1, x_2, x_3)-space. The surface plot has already been given in Figure 3. However, to get the more detailed view on structures of Ω_t we plot sections of Ω_t, m, g_1 and g_2 with respect to x_1 at $x_2 = 0$ plane. The two kinks are clearly visible at $t = 2.0$ and $t = 2.5$. The upper part of Ω_0 is clearly convex upward and rays diverge leading to a decrease in the value of m. However, near the base $x_3 = 0$, one principal curvature is positive but other negative. The kink lines are formed as circles. At $t = 2.5$ there appears to be a complex geometry near the upper kink circle as seen in Figures 9 and 11. It is interesting that the 3-D KCL are able to give such finer details.

Furthermore, it is worth remarking that the KCL reduce the original problem of evolution of Ω_t in four dimensions (x_1, x_2, x_3, t) to that in three dimensions in (ξ_1, ξ_2, t)-space. This reduces the computational cost considerably and hence many practical problems can be solved more efficiently.

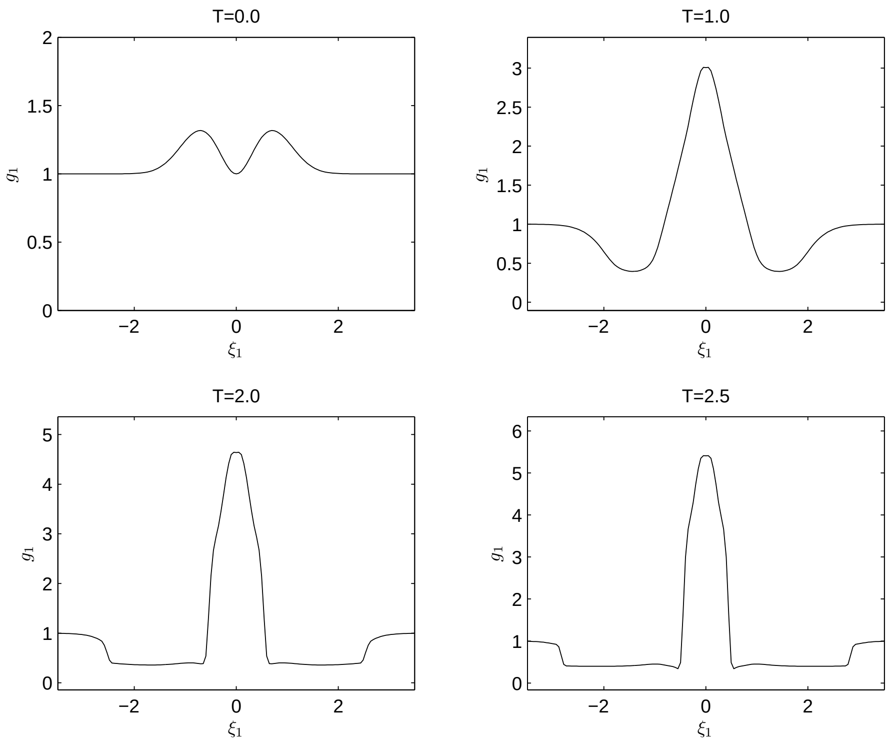

FIGURE 7. Time evolution of the metric g_1 at the cross-section $\xi_2 = 0$.

In the **second test case** an initial wavefront Ω_0 is taken to be an axi-symmetric paraboloid extended by a tangent conoid given in the following way

$$x_3 = \begin{cases} (x_1^2 + x_2^2)\,, & \text{if} \quad (x_1^2 + x_2^2)^{1/2} \leq 1, \\ 2(x_1^2 + x_2^2)^{1/2} - 1, & \text{otherwise.} \end{cases}$$

In [25] an analogous 2D-test problem has been considered. However, in 3D-case we have observed stronger singularity leading to numerical instabilities for large t. In Figure 13 the computational results obtained by the Lax-Friedrichs scheme up to $t = 1.5$ are presented. We have used a grid with 100×100 cells and had to set the CFL number to 0.15. We have approximated this problem also by the Nessyahu-Tadmor scheme. Due to less numerical viscosity the second order method gives comparable results only up to $t = 0.4$, afterwards it seems to be unstable. We do not give these results here as we like to investigate thoroughly the reasons of the failure of the Nessyahu-Tadmor scheme for this problem in future.

We have presented two illustrating numerical experiments showing that the 3-D KCL is a useful tool to study evolution of moving surfaces. First and second order central schemes have been applied to study the time evolution of a nonlinear wavefront which has initially both concave and convex parts. We have obtained some very interesting shapes of the wavefronts for two cases - in one case a kink line and another case a point singularity appear in the physical space though the results remain single valued in the ray coordinates, as expected for a system of conservation laws. The second example presents a new challenge which we shall study and report in subsequent papers. Our future goal is to investigate the propagation of a curved nonlinear wavefront where the converging effects and appearance of analogous singularities are dominant. This may lead to the formation of δ waves similar to δ shocks. In future our emphasis will be to study this situation more closely

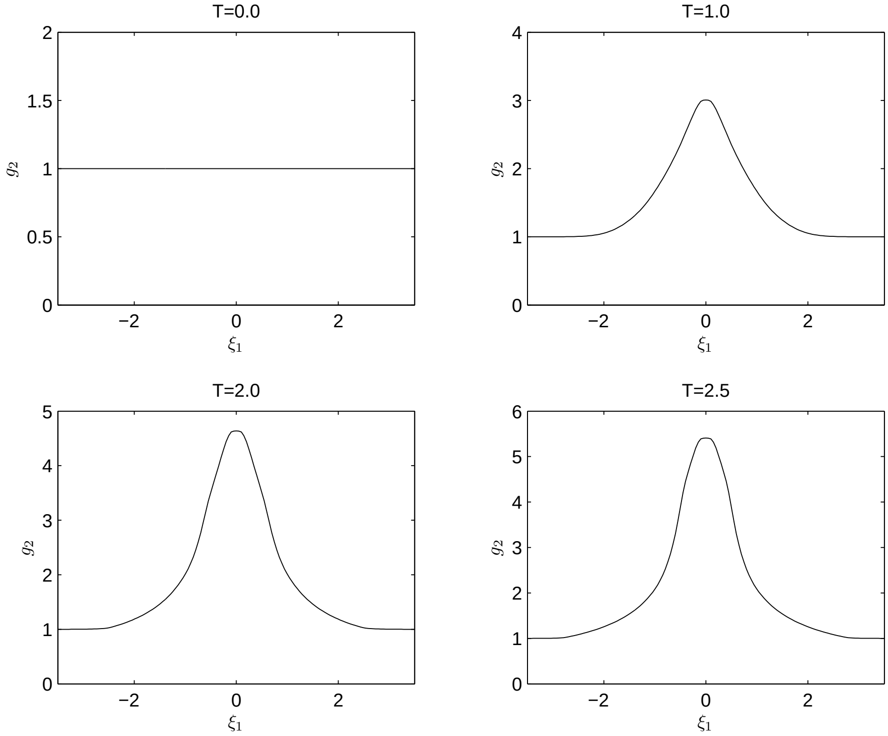

FIGURE 8. Time evolution of the metric g_2 at the cross-section $\xi_2 = 0$.

from theoretical as well as computational point of view and design robust and stable numerical algorithms.

Acknowledgement

We thank the Department of Science and Technology (DST), Government of India and the German Academic Exchange Service (DAAD) for the financial support of our collaborative research. Phoolan Prasad acknowledges financial support of the Department of Atomic Energy, Government of India under Raja Ramanna Fellowship Scheme. K. R. Arun would like to express his gratitude to the Council of Scientific & Industrial Research (CSIR) for supporting his research at the Indian Institute of Science under the grant-09/079(2084)/2006-EMR-1. Department of Mathematics of IISc is supported by UGC under SAP.

References

[1] P. Arminjon, M. C. Viallon and A. Madrane. A finite volume extension of the Lax-Friedrichs and Nessyahu-Tadmor schemes for conservation laws on unstructured grids. *Int. J. Comp. Fluid Dyn.* 9:1-22, 1997.

[2] K. R. Arun and P. Prasad. 3-D Kinematical Conservation Laws (KCL): Equations of evolution of a surface. *Preprint* No. 33, 2007, Department of Mathematics, Indian Institute of Science, Bangalore.

[3] S. Baskar and P. Prasad. Kinematical conservation laws applied to study geometrical shapes of a solitary wave. *Wind over waves II: Forcasting and Fundamentals.* S. Sajjadi and J. Hunt (eds.), Horwood Publishing Ltd, pp.189-200, 2003.

[4] S. Baskar and P. Prasad. Riemann problem for kinematical conservation laws and geometrical features of non-linear wavefronts. *IMA J. Appl. Math.* 69(4):391-420, 2004.

[5] S. Baskar and P. Prasad. Propagation of curved shock fronts using shock ray theory and comparison with other theories. *J. Fluid Mech.* 523:171-198, 2005.

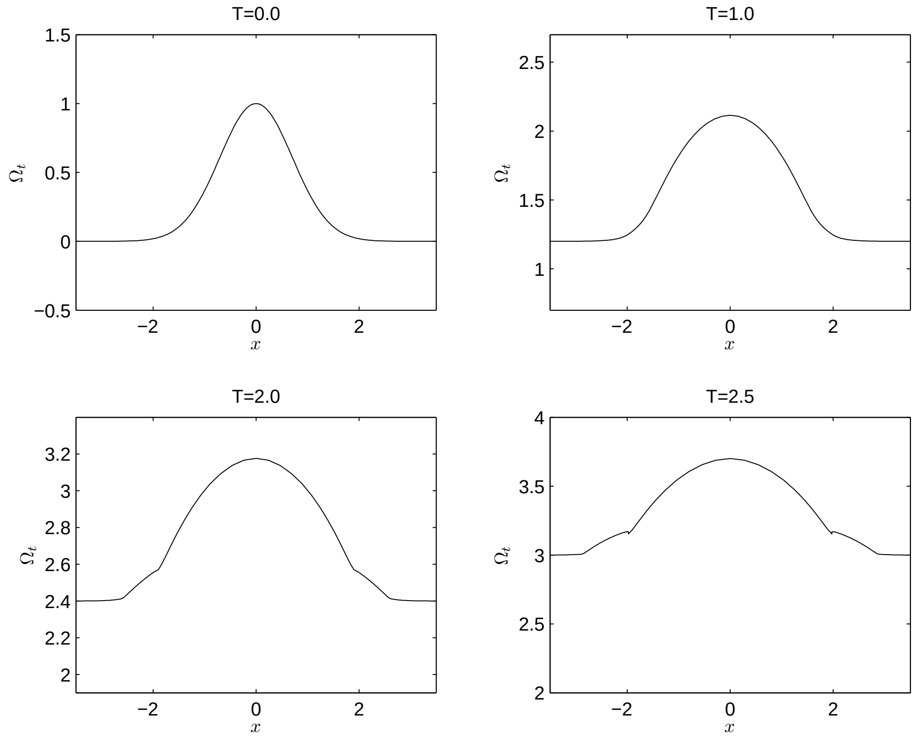

FIGURE 9. Time evolution of the geometry and position of the nonlinear wavefront Ω_t at cross-section $x_2 = 0$.

[6] S. Baskar and P. Prasad. Formulation of the problem of sonic boom by a maneuvering aerofoil as a one parameter family of Cauchy problems. *Proc. Indian Acad. Sci. (Math. Sci.)* 116:97-119, 2006.

[7] F. Bouchut. On zero pressure gas dynamics. In *Advances in Kinetic Theory and Computing*, volume 22 of *Ser. Adv. Math. Appl. Sci.*, pp.171-190. World Sci. Publishing, River Edge, NJ, 1994.

[8] F. Bouchut, S. Jin and X. Li. Numerical approximations of pressureles and isothermal gas dynamics, *SIAM J. Num. Anal.*, 41:135-158, 2003.

[9] Y. Brenier and E. Grenier. Sticky particles and scalar conservation laws. *SIAM J. Num. Anal.* 35:2317-2328, 1998.

[10] G. Q. Chen and P. T. Kan. Hyperbolic conservation laws with umbilic degeneracy (I). *Arch. Rat. Mech. Anal.* 130:231-276, 1995.

[11] R. Courant and F. John. Introduction to calculus and analysis, vol II. *John Wiley and Sons, New York,* 1974.

[12] R. Courant and K. O. Friedrichs. Supersonic flow and shockwaves. *Interscience Publishers, New York,* 1948.

[13] V. G. Danilov and D. Mitrovic. Delta shock wave formation in the case of triangular hyperbolic system of conservation laws. *to appear in J. Diff. Equations*, avialable on `http//www.math.ntnu.no/conservation/2006/057.html`

[14] B. Enquist and O. Runborg. Multi-phase computations in geometrical optics. *J. Comp. Appl. Math.* 74:175-192, 1996.

[15] M. Giles, P. Prasad and R. Ravindran. Conservation form of equations of three dimensional front propagation. *Technical Report, Department of Mathematics, Indian Institute of Science* 1995.

[16] F. Huang. Existence and uniqueness of discontinuous solutions for a class of nonstrictly hyperbolic systems, *Advances in Nonlinear Partial Differential Equations and Related Areas*, Beijing 1997, 187-208, World Sci. Publ., River Edje, NJ, 1998.

[17] G. S. Jiang and E. Tadmor. Nonoscillatory central schemes for multidimensional hyperbolic conservation laws. *SIAM J. Sci. Comp.* 19:1892-1917, 1995.

[18] G. S. Jiang, D. Levy, C. T. Lin, S. Osher and E. Tadmor. High-resolution nonoscillatory central schemes with nonstaggered grids for hyperbolic conservation laws. *SIAM J. Num. Anal.* 35:2147-2168, 1998.

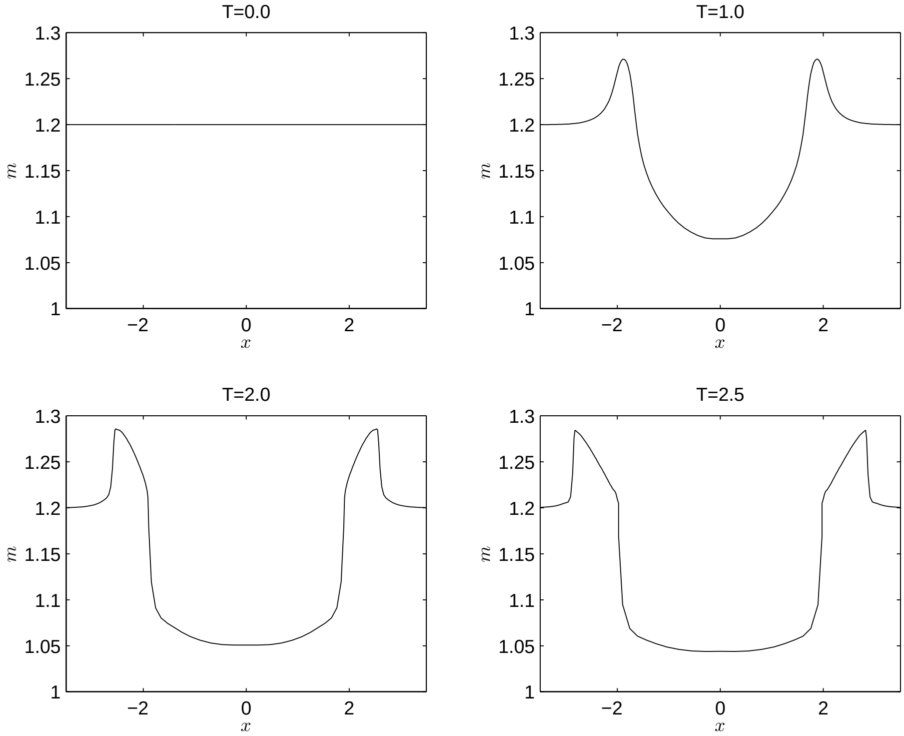

FIGURE 10. Time evolution of the normal velocity m at the cross-section $x_2 = 0$.

[19] P. Lax. Weak solutions of nonlinear hyperbolic equations and their numerical computation. *Comm. Pure Appl. Math.* 7:159-193, 1954.

[20] M. P. Lazarev, R. Ravindran and P. Prasad. Shock propagation in gas dynamics: explicit form of higher order compatibilty conditions. *Acta Mech.* 126:139-155, 1998.

[21] P. G. LeFloch. An existence and uniqueness result for two nonstrictly hyperbolic systems. *IMA Volumes in Math. and its Appl., "Nonlinear evolution equations that change type"*. B. L. Keyfitz and M. Shearer (eds.), Springer Verlag, Vol. 27, pp.126–138, 1990.

[22] R. J. LeVeque. The dynamics of pressureless dust clouds and delta waves. *J. Hyper. Diff. Equat.* 1: 315-327, 2004.

[23] T. P. Liu and Z. Zin. Stability of viscous shock waves associated with a system of nonstrictly hyperbolic conservations laws. *Commu. Pure Appl. Math.* 45:361-388, 2006.

[24] A. Majda and Y. Zheng. Existence of global weak solutions to one-component vlasov-poisson and fokker-planck-poisson systems in one space dimension with measures as initial data. *Commu. Pure Appl. Math.* 47:1365-1401, 2006.

[25] A. Monica and P. Prasad. Propagation of a curved weak shock. *J. Fluid Mech.* 434:119-151, 2001.

[26] K. W. Morton, P. Prasad and R. Ravindran. Conservation form of nonlinear ray equations. *Technical report No.2, Department of Mathematics, Indian Institute of Science Bangalore*. 1992.

[27] H. Nessyahu and E. Tadmor. Non-oscillatory central differencing for hyperbolic conservation laws. *J. Comp. Phys.* 87:408-463, 1990.

[28] P. Prasad. Nonlinear hyperbolic waves in multi-dimensions. *Monographs and Surveys in Pure and Applied Mathematics, Chapman and Hall/CRC, 121*, 2001.

[29] P. Prasad. Kinematical conservation laws, ray theories and applications. *Indian J. Pure and Appl. Math.* 38:467-490, 2007.

[30] P. Prasad and K. Sangeeta. Numerical simulation of converging nonlinear wavefronts. *J. Fluid Mech.* 385:1-20, 1999.

[31] V. M. Shelkovich. Multidimensional delta-shocks and the transportation and concentration processes. Preprint 2007, available on `http://www.math.ntnu.no/conservation/2007/031.html`

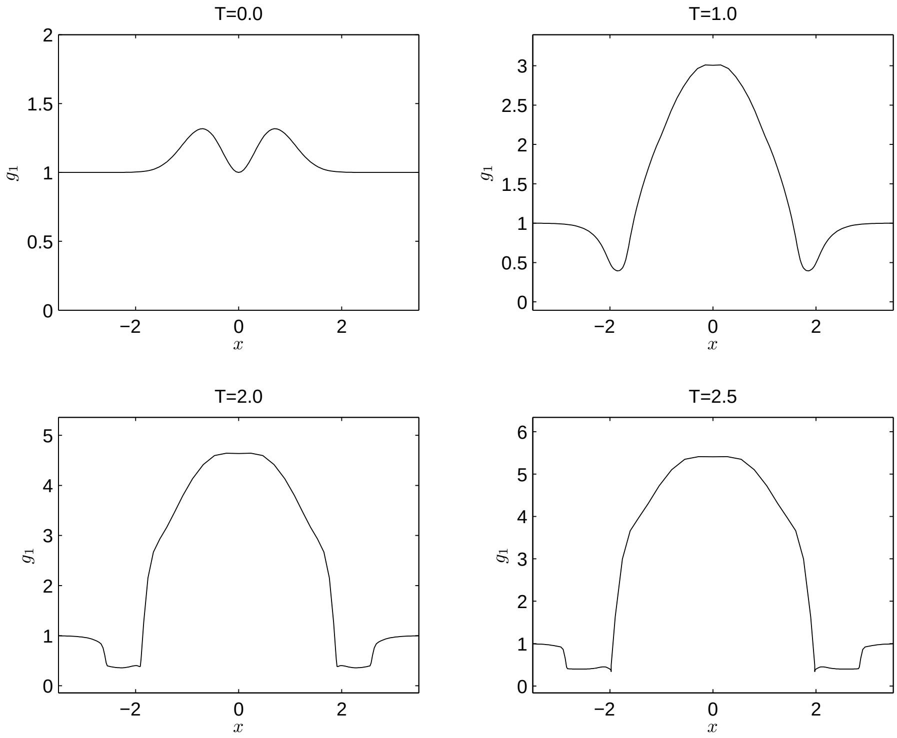

FIGURE 11. Time evolution of the metric g_1 at the cross-section $x_2 = 0$.

[32] O. Runborg. Some new results in multiphase geometrical optics. *M2AN Math. Model. Numer. Anal.* 34:1203-1231, 2000.

[33] D. Tan, T. Zhang and Y. Zheng. Delta-shock waves as limits of vanishing viscosity for hyperbolic systems of conservation laws. *J. Diff. Equations.* 112:1-32, 1994.

[34] G. B. Whitham. Linear and nonlinear waves. *John Wiley, New York,* 1974.

(K. R. Arun and Phoolan Prasad) Department of Mathematics, Indian Institute of Science, Bangalore, India-560012.

E-mail address: prasad@math.iisc.ernet.in

URL: http://math.iisc.ernet.in/~prasad/

(M. Lukáčová-Medviďová) Institute of Numerical Simulation, Hamburg University of Technology, D-21071 Hamburg, Germany.

E-mail address: lukacova@tu-harburg.de

URL: www.tu-harburg.de/ins/hp/lukacova/

(S. V. Raghurama Rao) Department of Aerospace Engineering, Indian Institute of Science, Bangalore, India-560012.

E-mail address: raghu@aero.iisc.ernet.in

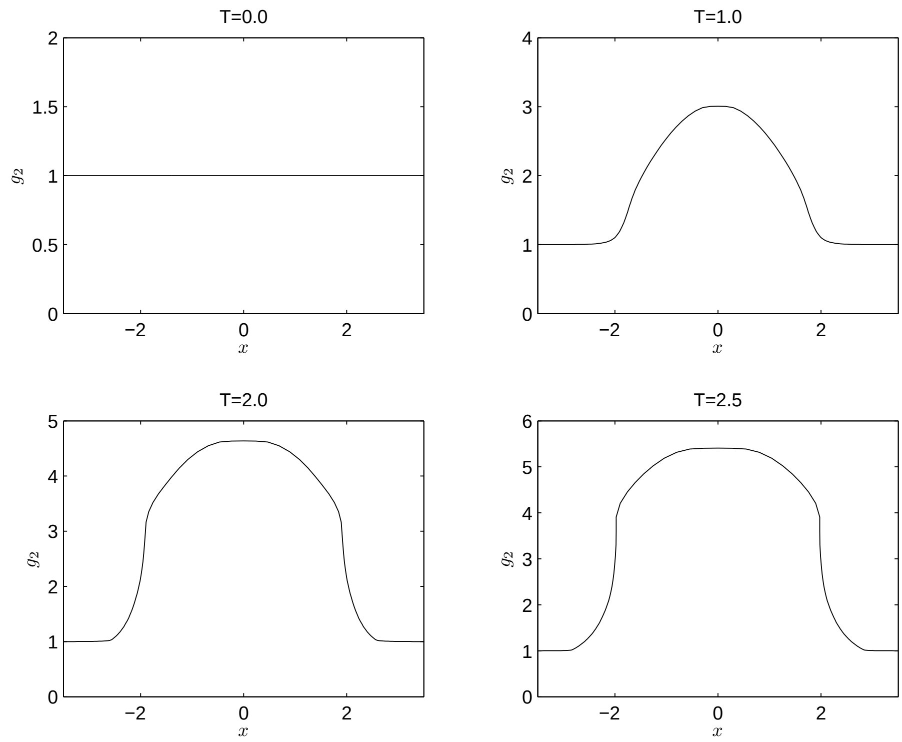

FIGURE 12. Time evolution of the metric g_2 at the cross-section $x_2 = 0$.

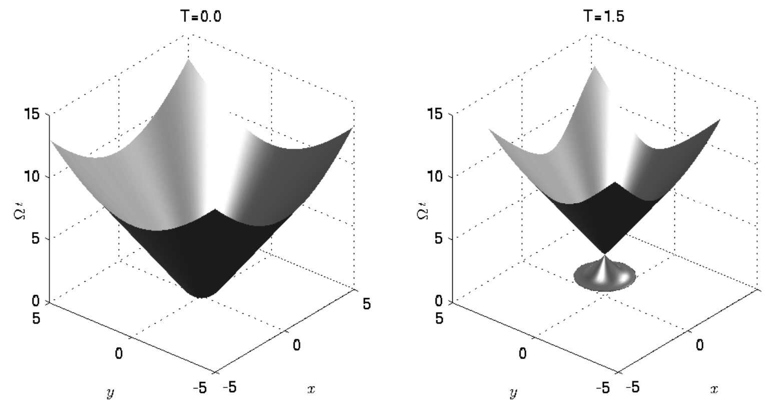

FIGURE 13. Time evolution of the nonlinear wavefront having initially the form of a paraboloid; graphs of solution at $t = 0.0$ and $t = 1.5$.